Formation of Gas Bubbles at Horizontal Orifices

LEON DAVIDSON and ERWIN H. AMICK, JR.

Columbia University, New York, New York

Air bubbles were formed in water and in mineral oil by use of single, circular, horizontal, square-edged orifices facing upward. Twenty orifices were tested, ranging from 0.017 to 0.79 cm. (0.0067 to 0.31 in.) in radius. Increasing the volume of the gas chamber below the orifice (over the range of 4 to 4,000 cc.) was found to increase the bubble size. The gas-chamber volume was minimized in most of the work in order to confine attention to the effects of orifice size and gas-flow rate. The liquid containers were large enough to eliminate significant wall effects, and operations were conducted at atmospheric pressure.

The gas-flow rate was varied from about 0.01 to about 250 cc./sec. over the course of the work. At relatively low flow rates, the orifices generally formed single "static" bubbles, the volumes of which were proportional to the surface tension and orifice radius and independent of the gas-flow rate. At high flow rates the bubble frequency became high and the bubble volume became proportional to the gas-flow rate and independent of the surface tension. The bubble frequency reached a maximum value for each orifice, this value being a function of the orifice radius. For air bubbles in water, the correlation of the maximum bubble frequency, n_m bubbles/sec., with the orifice radius, r cm., and the air-flow rate, q cc./sec., was found to be $n_m = 9.1q^{0.13}/r^{0.43}$. The maximum frequencies ranged from about 25 bubbles/sec. for the largest orifices to about 75 bubbles/sec. for the smallest orifices used.

It was found that consecutive bubbles paired or coalesced in definite ways in certain ranges of the gas-flow rate. A description is given of this bubble behavior, based on stroboscopic and photographic observation.

The interest of chemical engineers in studies of the formation of gas bubbles at orifices immersed in a liquid has grown tremendously since the 1946 paper of Geddes (*4*). Many recent papers include analytic treatment of the subject (*7, 9*) or correlate the phenomena involved (*11*). The present paper describes work done in 1949 at Columbia University in a series of bubble-formation experiments which covered a wide range of orifice diameters and gas-flow rates.

This study has been based on certain generally accepted simplifying assumptions and calculational procedures and has been limited to a reasonably small set of variables. The guiding principle has been that determinations of bubble volume and bubble frequency, as well as descriptions of bubble behavior, should be based on observations of a large number of consecutive bubbles formed under steady operating conditions. For convenience, the volumetric gas-flow rate (steady time-average value) was chosen as an independent variable, and the bubble volume and bubble frequency have been treated as dependent variables. Orifice radius has been a major variable in this study, covering a fortyfold range of values. As a linear measure of the "size" of a gas bubble, the radius of a sphere having an equal volume has been used.

The usual simplifying conditions, which were satisfied in the present work, are that there is no chemical reaction between the gas and the liquid and that the liquid container is wide enough to preclude wall effects. Procedures were simplified by operating at essentially atmospheric pressure and using air as the gas phase, since the physical properties of the gas are assumed to enter the theory in simple and readily calculable ways.

Single, circular, horizontal, square-edged orifices were used, generally mounted essentially flush with the bottom of the liquid container, facing upward. The volume of the gas chamber below the orifice is considered to include the entire gas volume in the piping extending back to the nearest effective restriction governing the air flow through the orifice.

In the present work it was found that container widths from 3 to 10 in. square had no effect and that orifice submergences from about 1 to about 10 in. usually had negligible effect. When the orifice projected above the container bottom (as for a capillary-type orifice), the bubble frequency was found to increase owing to the enhanced liquid circulation, in agreement with the results of Maier (*8*) and Sprague (*10*). No results for such a case will be discussed in this paper, but the effect of the orifice-chamber volume will be discussed.

The analysis of the bubble-formation problem by van Krevelen and Hoftijzer (*11*), otherwise similar to that followed in the present work, omitted the orifice radius as a factor in the high-bubble-frequency region. This probably resulted from the fact that those authors did not have available to them any high-frequency data for orifices larger than 0.025 cm. in radius.

APPARATUS AND TECHNIQUES

A constant-pressure air-supply system was of vital importance in enabling extremely reproducible data and photographs to be obtained. It consisted of a diaphragm-type pressure regulator (reducing the laboratory air supply from about 55 to about 25 lb./sq. in. gauge) followed by a sensitive needle valve for flow regulation (dropping the pressure from about 25 to about 2 lb./sq. in. gauge). A separate shut-off valve following the needle valve permitted the flow setting to remain undisturbed between parts of a run, if required. Despite fluctuating line pressure, this system gave extremely steady performance owing to the constant upstream pressure maintained on the critical-pressure-drop needle valve. (*See* the section Reproducibility of the Data below.)

A capillary flow meter was used, with two interchangeable capillaries providing a usable range from 3 to 250 cc./sec. It was operated at a constant upstream pressure of 880 mm. Hg absolute. At very low flow rates the bubble frequency, bubble volume, and air-flow rate were determined by collec-

Leon Davidson is at present with Nuclear Development Corporation of America, White Plains, New York.

Table 1. Inside Radii of the Orifices Used in the Present Work

Orifice	r, cm.	Orifice	r, cm.	Orifice	r, cm.	Orifice	r, cm.	Length, cm.*
A-1	0.35	*B*-1	0.48	*C*-2	0.79	*D*-1	0.20	0.32
A-2*a*	0.16	*B*-2	0.40	*C*-3	0.64	*D*-2	0.21	1.27
A-3*a*	0.08	*B*-3	0.32	*C*-4	0.56	*D*-3	0.21	2.54
A-4	0.048	*B*-4	0.16	*C*-61	0.05	*D*-4	0.05	0.32
A-5	0.017	*B*-5	0.05	*C*-71	0.017	*D*-5	0.40	7.6

*All orifices except the *D* series were holes drilled in brass plates 0.08 cm. thick. The *D* series were sections of tubing of the lengths listed.

tion of a counted number of bubbles in a graduated cylinder for a timed interval.

The liquid containers, made of cellulose acetate, had flat sides 1 ft. high and 3 to 10 in. wide, cemented to a brass base plate. Under the center of the plate a fitting was provided for mounting the orifices.

The orifices used are described in Table 1. The orifices of series *A*, *B*, and *C* were made by drilling single holes in thin brass sheets and soldering these over the ends of brass or copper tubes of somewhat larger diameter than the holes. Series *D* consisted simply of sections of brass or copper tubing having one end faced off squarely to act as the orifice. The orifice tubes were supplied with air through a tee which during certain runs allowed any liquid which dripped down through the orifice to be automatically siphoned off and measured, without affecting the air-flow rate or the chamber volume.

At higher frequencies than could be directly counted, a General Radio Company Strobotac was used, with the room darkened, to "stop" the motion of the bubbles. The Strobotac was also used to allow slow-motion studies of bubble behavior. A scale on this instrument gave the bubble frequency directly when the bubbles appeared to be "stopped" at the orifice. The steadiness of the air-supply system made this technique quite feasible and allowed readings to be made rapidly. Suitable means were utilized to assure that the correct frequency was determined. For example, since the true bubble frequency and the vertical spacing between single bubbles were essentially constant during a run, the apparent spacing between the bubbles would be halved when the Strobotac frequency was increased to twice the correct bubble frequency. The apparent spacing, however, would remain equal to the true spacing when the Strobotac frequency was decreased to one-half the true bubble frequency, but in the latter case the visual image was noticeably dimmer, as there were only half as many illumination periods per second.

In some runs electronic flash photographs were taken to record typical bubble behavior, but these were not used as a source of quantitative data. Data derived from the various instruments or techniques checked and overlapped quite well, and so there is a negligible possibility that breaks in the curves can be attributed to instrument errors.

TYPES OF BUBBLE FORMATION

As has been pointed out by van Krevelen and Hoftijzer (*11*), two distinct regimens of bubble formation are found to occur as the gas-flow rate through an orifice is increased. At very low flow rates (and with a reasonably small gas-chamber volume below the orifice) the bubble volume is predicted within a factor of two by the hydrostatic equation

$$v_s = \frac{2\pi r\sigma}{(\rho - \rho_g)g} \qquad (1)$$

The bubble volume remains constant at about the value given by Equation (1), independent of moderate changes in the gas-flow rate, and so the bubble frequency is proportional to the gas-flow rate in this range. This may be referred to as the region of *constant-volume* or *static* bubbles.

As the gas-flow rate increases sufficiently, it is found that the bubble frequency levels off at a constant value and that the bubble volume thereafter increases in proportion to the gas-flow rate. This may be called the region of *constant-frequency* bubbles. It is this region which will prove to be of most interest in this paper.

CONSTANT-VOLUME BUBBLE REGION

Possible refinements of Equation (1) might be considered to improve its imperfect fit to the experimental data. A factor might be included to allow for the increase in bubble volume with large chamber volumes below the orifice, as discussed by Hughes et al. (*7*). A factor might also be included to account for the deviation of the bubble profile from the true vertical, where it is attached to the orifice, since Equation (1) assumes a vertical profile. Wark (*12*) discussed the relationship for stationary bubbles between the angle of contact of the gas-water-solid interfaces and the bubble volume. His theoretically calculated profiles agree well with observations.

The relation between the radius of the detached "static" bubble and the orifice radius, which may be derived from Equation (1), is

$$\frac{a}{r} = \left(\frac{1.5\sigma}{r^2(\rho - \rho_g)g}\right)^{1/3} \qquad (2)$$

where a = radius of equivalent spherical bubble, cm. Thus, as the orifice size increases, the static-bubble radius will eventually become smaller than the orifice radius. The gas-liquid interface will then tend to be horizontal at the orifice perimeter, leading to instability. In this work stable stationary bubbles could not be formed at an orifice having a radius of 0.79 cm. (0.31 in.), but stable bubbles were formed at an orifice of 0.64-cm. radius (0.25 in.). It may be concluded that orifices larger than about 0.7-cm. radius (0.27 in.) cannot produce stable static bubbles in water.

It might be worth noting that for very viscous liquids [for example, the castor oil and olive oil of Guyer and Peterhans (*5*)] even such a low frequency as one bubble per second may be far above the static-bubble flow-rate range and may be well in the region where bubble volume is increasing with gas-flow rate.

EFFECT OF THE VOLUME OF THE ORIFICE CHAMBER

A series of runs was made to determine the effect of the volume of the gas space below the orifice (the "chamber volume"), using single orifices of 0.16-cm. (0.063 in.) radius over a wide range of flow rates. The data are shown in Figure 1. The chamber volume ranged from about 4 to about 4,000 cc., corresponding to values of the "capacitance number" N_c ranging from 0.033 to 33.0. N_c is a parameter developed by Hughes et al. (*7*) relating the acoustical properties of the gas-orifice system to the chamber volume, as follows:

$$N_c = \frac{g(\rho - \rho_g)V_b}{\pi r^2 \rho_g c^2} \qquad (3)$$

where

V_b = volume of chamber below orifice, including gas lines, cc.

c = velocity of sound in the gas, cm./sec.

In agreement with the results of Hughes, the bubble behavior was found to be independent of N_c for $N_c < 0.8$, at low flow rates. At higher flow rates the critical value of N_c decreased to about 0.2. In the bulk of the present work the chamber volume was minimized to eliminate its effect.

In the region of large chamber volumes, to the right of the dashed line on Figure 1, indicated by the word *pair*, the ordinate value plotted is the combined volume of the pair of bubbles released at one time. It is very important to note that this type of bubble pairing, which is characteristic of large chamber volumes, is definitely not the same type of bubble pairing as will be described below under Transition Region. The pairing now under discussion may occur even at very low flow rates for a given orifice, as Figure 1 shows, before the transition region is reached. This type of "pair creation" is caused by the surplus gas accumulated in the chamber volume between bubble-release times. It is more fully discussed, from the theoretical and experimental aspects, in Sections 2.6 and 7.7 of the original thesis (*2*). Hughes et al. (*7a*) also discuss this.

BUBBLE-BEHAVIOR DATA FOR A TYPICAL ORIFICE

Typical plots of bubble frequency and bubble volume vs. gas-flow rate for a flat-plate orifice are shown in Figures 2 and 3. The points represent results from four different arrangements using orifice *B*-4 over a period of several months. The orifice radius was 0.16 cm., and N_c was kept below 0.2. Data were obtained for both water and mineral oil. The letters on the plots indicate the regions in which certain phenomena occurred, to be described in the following paragraphs. This orifice was chosen for discussion because it demonstrated most of the interesting phenomena observed during the work. With other-size orifices some regions did not appear.

Static-bubbling Region

The value of v_e computed by Equation (1) is indicated on the bubble volume plot, Figure 3. While there is fair agreement, the bubble volume increases slightly with the flow rate, and the frequency is therefore slightly less than proportional to the flow rate.

Since the velocity of rise of bubbles is a function of their size (*11*), it is essentially constant in this region. Therefore for a given orifice the center-to-center spacing of the rising bubbles is inversely proportional to their frequency. At low frequencies the liquid at the orifice may be assumed to come to rest before each bubble escapes. The bubbles are identical at any given point early in their rising path. Although each bubble passes through violent symmetrical oscillations in shape as it rises, these are exactly copied by each succeeding bubble. Higher up, away from the stabilizing influence of the base plate, the bubbles move erratically sidewise and become irregular in shape.

Transition Region

At higher flow rates the bubble volume increases sharply as the frequency levels off. The spacing between bubbles has decreased, and each forming bubble is affected by the presence of the preceding bubble, perhaps through the mechanism of a liquid vortex ring at the orifice. The bubbles now start to form into pairs, although still forming individually at regular time intervals at the orifice. A bubble will appear to hover above the orifice until the next bubble emerges, and the two bubbles will then remain together as they rise. This pattern is repeated by the next two bubbles, and so on indefinitely.

In some cases pair formation as just described continues for only a fraction of a minute (during which time hundreds of bubbles form). The flow then suddenly reverts to single-bubble formation, at a bubble frequency about 5 to 30% higher than existed during the period of pair formation. These single bubbles are usually elongated and twisted, like candle flames, and show turbulence and erratic behavior even near the orifice. After a fraction of a minute pair formation begins again. The flow oscillates periodically between the two regimens. However, the bubble frequency in a given regimen returns to the same value each time that that regimen is restored. Gas-flow rate remains constant. (One might speculate that the two regimens correspond to two different states of liquid motion in the vicinity of the orifice, e.g., axially symmetrical pulsating flow in the case of pair formation and continuous rotation about the orifice axis in the case of the twisted single bubbles.)

Bubble frequencies reported in this transition region are averages for the two regimens. Scatter of the data in this region is due partly to persistence of one or the other regimen throughout certain runs, which introduces the frequency difference between the regimens into the results.

Incipient Coalescence

As the flow rate further increases, the members of a bubble pair touch each other. This condition may be called

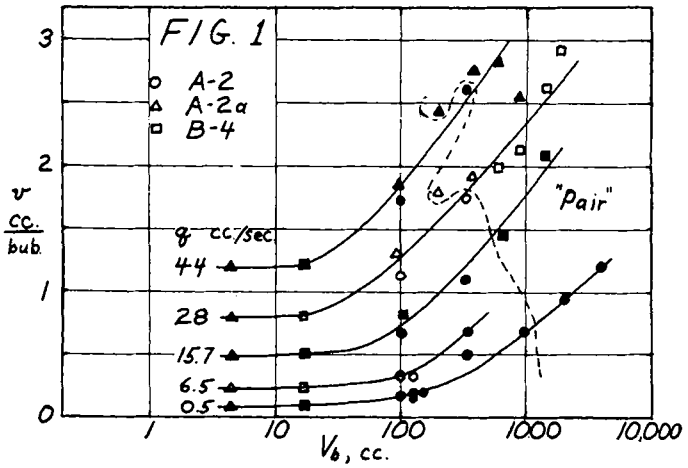

Fig. 1. Bubble volumes v vs. volume of chamber below orifice V_b at various air flow rates q for orifices having radii of 0.16 cm. (air-water data). In the region marked "pair" to the right of the dashed line, v is the combined volume of the pair of bubbles emitted at one time.

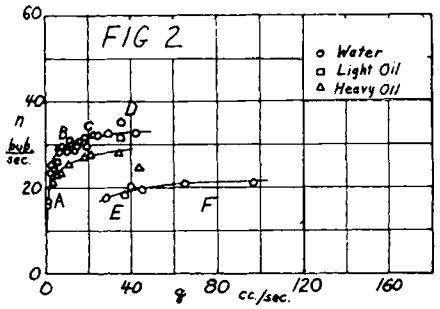

Fig. 2. Bubble frequency n vs. air flow rate q for orifice *B*-4; orifice radius 0.16 cm., container width 12 cm., liquid depth 5 to 10 cm., chamber volume 10 to 17 cc. (data for air-water and air-oil systems). The letters refer to regions of static bubbling (*A*), transition (*B*), incipient coalescence (*C*), coalescence (*D*), coalescence at the orifice (*E*), and double coalescence (*F*).

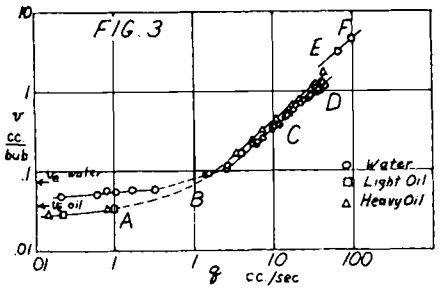

Fig. 3. Bubble volume v vs. air flow rate q for orifice *B*-4; orifice radius 0.16 cm., container width 12 cm., liquid depth 5 to 10 cm., chamber volume 10 to 17 cc. (data for air-water and air-oil systems). The letters refer to regions given under Figure 2.

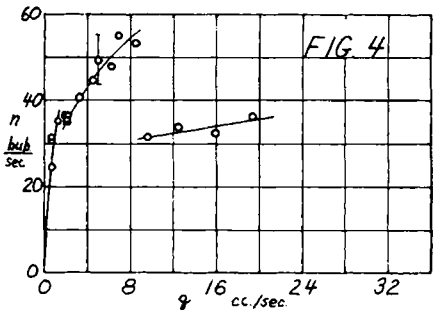

Fig. 4. Bubble frequency n vs. air flow rate q for orifice *C*-61; orifice radius 0.05 cm., container width 12 cm., liquid depth 10 cm., chamber volume 2.9 to 4.4 cc. (air-water data).

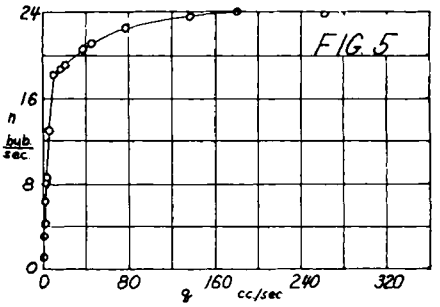

Fig. 5. Bubble frequency n vs. air flow rate q for orifice *B*-1; orifice radius 0.48 cm., container width 12 cm., liquid depth 10 cm., chamber volume 22 cc. (air-water data).

Table 2. Examples of Reproducibility of Data for Air Bubbles in Water
(With minimized volume of chamber below the orifice)

Orifice	Run	Air flow, cc./sec., q	Bubbles/ sec., n	Actual Strobotac frequency readings during run, single bubbles/min.
A-2a	43–19	1.249	15.0	905, 898, 895, 900, 900
A-2a	43–20	1.246	14.9	895, 898, 885, 885, 892, 892
A-2a	43–21	1.238	14.9	898, 892, 895, 895, 894
A-2a	43–22	1.235	15.0	895, 899, 905, 895, 898
A-2a	43–23	1.260	15.0	897, 899, 910, 895, 897, 895
B-4	33–7	11.5	31.0	1,830*, 1,945, 1,765, 1,930*, 1,840*
B-4	33–13	11.5	30.4	1,800*, 1,780, 1,888, 1,900*, 1,750*

*These values are reported as exactly twice the actual value recorded experimentally, which corresponded to the frequency of doublet formation in these particular cases.

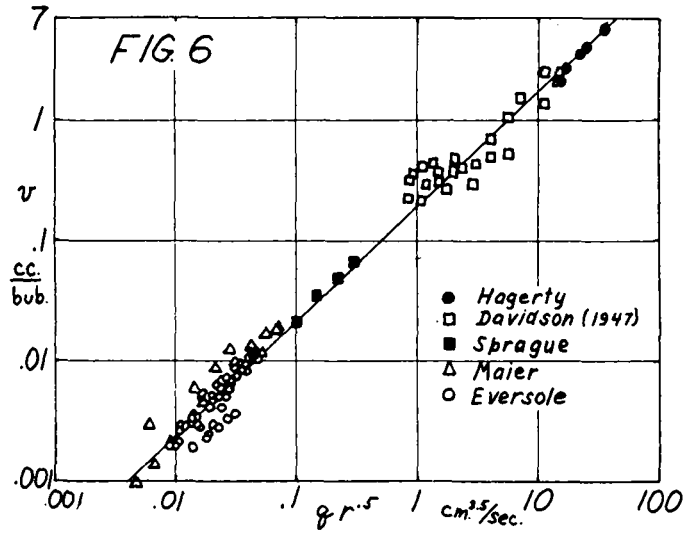

Fig. 6. Correlation of bubble volume v vs. (gas flow rate times square root of orifice radius) $qr^{0.5}$ for literature data in the constant-frequency region. The line drawn in has the equation $v = 0.19(qr^{0.5})^{0.95}$.

"doublet formation." The first member of the doublet usually assumes a hemispherical shape, and the second bubble is elongated vertically; the assembly resembles a mushroom. (The similarity between this behavior and the behavior of rising balls of fire, including atomic-bomb explosions, suggests that some common underlying principle is involved, since the fireball is merely a bubble of low-density gas in an atmosphere of higher density.)

With higher flow rates, the lower bubble often momentarily protrudes into the top bubble. This protrusion is facilitated by a column of liquid which rises inside the top bubble.

Coalescence

Further flow-rate increase causes the second bubble to penetrate the first one appreciably. Under some conditions the second bubble always shoots completely through the first bubble, rising through the inner column of liquid in the bubble and emerging on top. Under other conditions the first bubble absorbs part of the second and leaves the residue as a small satellite. In still other cases the second bubble is completely swallowed by the first, although their interface remains unruptured.

In most cases, however, the two bubbles completely coalesce at these flow rates, at some distance above the orifice, yielding a single large irregular bubble. At this point the frequency has usually reached a maximum value which remains essentially constant as the flow rate increases further. Liquid viscosity and orifice radius seem to have some effect on the value of the constant frequency.

Coalescence at the Orifice

Coalescence takes place closer and closer to the orifice as the flow rate increases. A flow rate is finally reached at which the bubbles coalesce right at the orifice, the first bubble having no time to rise before the second one emerges. Under these conditions it will appear that the frequency of bubbles rising from the orifice has suddenly been halved.

Double Coalescence

As the flow rate further increases, the large coalesced bubbles themselves undergo coalescence as they rise. This may be called "double coalescence." At this stage the fluid is usually quite turbulent and the gas seems to issue from the orifice as a continuous jet. The bubbles are erratic, and good data are hard to obtain. The liquid becomes filled with small circulating bubbles. At this point conditions of industrial interest are undoubtedly approached, but unfortunately this is the point at which laboratory experiments usually have to be terminated.

CURVES FOR OTHER ORIFICES

In the original thesis describing this work (*2*) are complete plots of the data for about twenty orifices, as listed in Table 1. A few of these plots are reproduced here. In Figure 4 the point plotted at $q = 5$ cc./sec. indicates the actual extreme values assumed by the frequency at that flow rate (in the transition region) as the flow regimen fluctuated between pair and single-bubble formation. Figure 5 shows data for a large orifice of 0.48-cm. radius. It is apparent that the maximum bubble frequency varies somehow inversely with orifice radius.

REPRODUCIBILITY OF THE DATA

Table 2 illustrates the reproducibility of the data for five consecutive runs with orifice *A-2a* at a constant flow setting, each run lasting several minutes. The individual Strobotac frequency readings were taken in the order given, at approximately quarter-minute intervals, and no single reading deviates by more than about 1% of the mean value for its particular run. The average frequencies for each of the five runs lie within 1% of each other also. Table 2 also illustrates the reproducibility of nonconsecutive runs for orifice *B*-4 at a given flow rate, which happens to lie in the transition region of Figure 2. The preceding discussion of the transition region will explain the increased scatter (up to 5%) in these individual Strobotac readings for orifice *B*-4, although even here the average bubble frequency does not differ by more than 2% between the two runs listed.

CORRELATION OF BUBBLE VOLUMES FROM LITERATURE DATA

Most of the data of Eversole et al. (*3*) are in the constant-frequency range, as are some data of Maier (*8*), Sprague (*10*), Hagerty (*6*), and Davidson (*1*). These data form lines of almost 45° inclination on logarithmic plots of bubble volume vs. flow rate for each orifice, but the various orifices do not line up well together on such plots. It was found empirically that by multiplying the flow rates by the square root of the orifice radius, a correlation could be obtained as shown in Figure 6, in which the data for a wide range of orifices line up well. No theoretical derivation of this correlating factor has been developed, but some ideas on the subject will be given later.

The relationship between bubble volume, flow rate, and orifice radius in the constant-frequency region appears from Figure 6 to be of the form

$$v = K(qr^{0.5})^w \qquad (4)$$

where

w = slope of straight line on a logarithmic plot

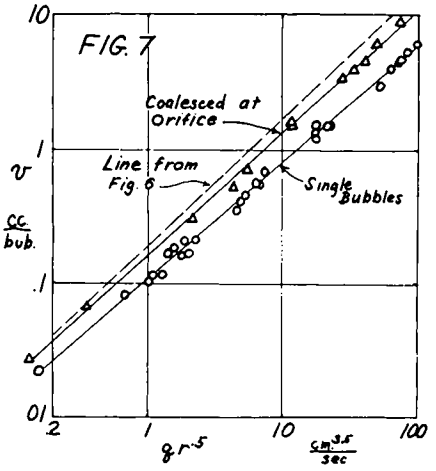

Fig. 7. Correlation of bubble volume v vs. (air flow rate times square root of orifice radius) $qr^{0.5}$ for present data in the constant-frequency region. The points plotted are the end points of the respective straight-line portions of the plots for the individual orifices.

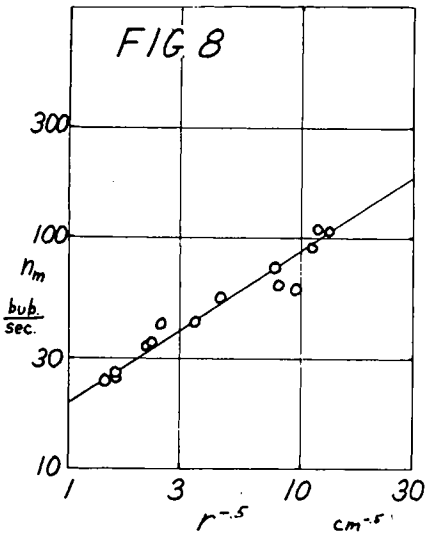

Fig. 8. Constant (maximum) bubble frequency n_m vs. reciprocal of square root of orifice radius $r^{-0.5}$ for the data of Table 3. The line drawn in has the equation $n_m = 19(r^{-0.5})^{0.66} = 19r^{-0.33}$.

K = value of ordinate of line at unity abscissa value

For the literature data plotted in Figure 6 the equation of the correlation line shown is

$$v = 0.189(qr^{0.5})^{0.953} \qquad (5)$$

CORRELATION OF THE BUBBLE-VOLUME DATA FROM THE PRESENT WORK

Data were available from the present work for thirteen orifices with radii from 0.0175 to 0.48 cm., with low values of N_c. Distilled water was the liquid chiefly used, but some data were obtained for light mineral oil ($\rho = 0.843$, $\sigma = 30.4$, viscosity = 0.224 poise) and for heavy mineral oil ($\rho = 0.861$, $\sigma = 31.2$, viscosity = 0.475 poise). The coordinates of the end points of the straight-line 45° portions of the individual orifice plots of bubble volume (similar to Figure 3) were read off and replotted on Figure 7 as bubble volume vs. $qr^{0.5}$. The correlation seems to be as good as that in Figure 6 for the literature data. The equation of the line marked *single bubbles* is

$$v = 0.110(qr^{0.5})^{0.867} \qquad (6)$$

For those orifices for which the halved bubble frequency was recorded, owing to coalescence at the orifice, the individual orifice plots show two parallel 45° lines at high flow rates, as in Figure 3 (where line EF is parallel to line CD but shows twice the bubble volume). In Figure 7 the end points of these upper lines from the individual orifice plots have been plotted as triangles. They form another correlation line roughly parallel to the main line but lying above it at about twice the bubble volume for a given abscissa value. The equation of this line, which is marked *coalesced at orifice*, is

$$v = 0.163(qr^{0.5})^{0.914} \qquad (7)$$

The literature-correlation line of Figure 6, copied onto Figure 7 as indicated, lies quite close to the line for the present data on bubbles which are coalesced at orifice. This suggests that the values given in the literature are chiefly for such coalesced bubbles. It is indeed found that the data of Maier (*8*) and Eversole (*3*) contain examples of bubble frequencies which are twice the usual values reported by those investigators. Probably these high frequencies correspond to the maximum single-bubble frequency, as in region D of Figure 2, and the remainder of the literature-data frequencies correspond to the halved frequency, as in the region of coalescence at the orifice.

CORRELATION OF THE MAXIMUM BUBBLE FREQUENCY

By dividing each side of Equation 4 into q, the flow rate, one obtains an expression for the constant (maximum) bubble frequency

$$n_m = \frac{q^{(1-w)}}{Kr^{0.5w}} \qquad (8)$$

For the data of this research for single bubbles, the corresponding expression, derived from the correlation of experimental data represented by Equation (6), is

$$n_m = \frac{9.09q^{0.133}}{r^{0.434}} \qquad (9)$$

It is evident that the maximum frequency, n_m, is not entirely a function of the orifice radius alone, but tends to increase slightly at the higher flow rates.

To shed further light on this, approximate values of q_m, the flow rate at which the maximum frequency first occurs for each orifice, were read off from plots of n vs. q (similar to Figures 2, 4, and 5). These q_m values are listed in Table 3, for orifices both from the literature and from the present work. It is seen that q_m increases substantially as r increases. Examination of Equation (9) indicates that if n_m were to be studied as a function of r only, the exponent of r would be effectively decreased in absolute value because of the offsetting nature of this variation in q_m.

This is illustrated in Figure 8, in which the constant-frequency data of Table 3 are plotted as a function of r only, the function chosen for the abscissa being the reciprocal square root of r. (Four cases in Table 3 were adjusted as indicated in the table to convert "coalesced-bubble" frequencies to single-bubble frequencies, as discussed previously.) The equation of the line drawn through the points on Figure 8 is

$$n_m = \frac{19}{(r^{0.5})^{0.67}} = \frac{19}{r^{0.33}} \qquad (10)$$

In agreement with the conclusion of the preceding paragraph, the exponent of r in

Table 3. Constant (Maximum)-bubble-frequency Data for Water

Reference or orifice	Orifice radius r, cm.	Bubble radius a, cm.	$\frac{a}{r}$	Capacitance number N_c	Maximum frequency, bubbles/sec. Obs.	Doubled	Calc. by Eq. (13)	q_m
Maier	0.00591	0.052	8.8	——	107	—	—	0.06
Maier	0.0075	0.092	12.2	——	54	108	—	≈0.2
Eversole*	0.0085	0.077	9.1	54	90	—	—	0.17
Maier	0.01125	0.105	9.3	——	30	60	—	0.2
Sprague	0.016	0.111	7.0	——	31	62	—	0.4
C-71	0.0175	0.159	9.1	2.1	74	—	60	1.0
D-4	0.050	0.166	3.3	0.39	55	—	36	9.
C-61	0.050	0.153	3.1	0.38	55	—	36	8.
A-3*a*	0.082	0.464	5.7	0.14	43	—	28	18.
A-2*a*	0.16	0.640	4.0	0.036	42	—	20	60.
D-1	0.20	0.701	3.5	0.057	35	—	18	60.
D-3	0.21	0.695	3.2	0.047	33	—	17	≈50.
Hagerty	0.395	0.683	1.7	0.15	13	26	—	60.
D-5	0.40	1.016	2.6	0.015	25	—	13	120.
B-1	0.48	1.020	2.1	0.02	24	—	12	160

*This was Eversole's point for 70% ethanol in water.

Equation (10) is smaller in absolute value than it is in Equation (9).

It must be considered therefore that although the maximum bubble frequency is a function of the orifice radius, it is not a function of that alone. However, for practical purposes it may be considered to be only a function of r (for liquids with comparable kinematic viscosities) because of the small exponent of q in Equation (9), and because q_m is a function of r. It is therefore believed that Equation (10) may be used to estimate the maximum individual bubble frequency for orifices in the range of 0.01- to 0.50-cm. radius for liquids with kinematic viscosities about the same as the viscosity of water. [*See* Section 8.7 of the original thesis (*2*) for a discussion of the effect of liquid viscosity.] The frequency given by Equation (10) should be halved to allow for the coalescence of bubbles at the orifice when that is expected to occur.

DISCUSSION OF THE MAXIMUM-FREQUENCY CORRELATION

By use of van Krevelen's working hypothesis (*11*) that at the maximum frequency bubbles are spheres which just touch each other in a vertical line above the orifice and of his correlation for the rising velocity of bubbles in series, which reduces to

$$V = (ag)^{0.5} \qquad (11)$$

where V = velocity of rise of bubbles in series, cm./sec., an equation relating orifice size and maximum frequency may be derived. From the data of Table 3 it is seen that at the maximum frequency the bubble radius is very roughly four times the orifice radius, over a wide range of orifice radii. Then, since by van Krevelen's hypothesis

$$V = 2an_m \qquad (12)$$

it follows that

$$n_m \approx \frac{8}{r^{0.5}} \qquad (13)$$

Values of n_m computed by Equation (13) are given in Table 3. The agreement with experiment is not good, because the real bubbles are far from being perfect spheres which just touch each other in a vertical line. Hence Equation (13) should not be used for predictions; it merely serves to illustrate a possible semitheoretical derivation of a correlation based on the square root of the orifice radius.

The relation of the maximum bubble frequency to the orifice radius should be tested by other investigators. The orifice radius was omitted as a factor in the analysis of van Krevelen (*11*). Equation (11) in his paper, for the critical gas flow rate, reduces to

$$n_m = \frac{36.5}{q^{0.2}} \qquad (14)$$

This equation, which indicates that the constant frequency is independent of the orifice size, does not agree with the data for large orifices and should not be used.

DIMENSIONAL CONSIDERATIONS

The correlation function, $qr^{0.5}$, which appears in Equation (4), was found empirically, but it appears to hold some promise of having theoretical significance. Dimensionally, Equation (4) is badly unbalanced, but it may be greatly improved by the reasonable assumption that an appropriate factor, having a practically constant numerical value, is concealed in the numerical constant K. The expression $g^{0.5}$ is just such a factor, where g is the local acceleration of gravity. Support for the choice of this factor, and an indication of the possible role it may play in the theoretical development, is found in the simple equation for the velocity of a freely falling body, which contains the same factor $g^{0.5}$:

$$u = (2gh)^{0.5} \qquad (15)$$

where

u = velocity of falling body, cm./sec.
h = distance through which body has fallen from rest, cm.

Writing the factor $g^{0.5}$ explicitly into Equation (4) (actually the more convenient and almost equal factor $g^{0.5w}$ is used) leads to the following equation:

$$v = K'\left(\frac{qr^{0.5}}{g^{0.5}}\right)^w \qquad (16)$$

where K' = changed numerical value of the constant K of Equation (4). The dimensions of the left member of Equation (16) are [length]^3, while on the right the dimensions are now [length]^{3w}. Since w is not quite equal to unity, although almost so, there remains a slight discrepancy in the dimensional balance of Equation (16). Probably, since Equation (4) was derived from an empirical study of the data, one or more other factors remain hidden in K' and contribute to the discrepancy. This remains to be determined from further work along these lines. (It is of course unnecessary to take specific account of this factor $g^{0.5}$ in the numerical calculations and plots, as it has a constant value for all practical purposes and is covered by the numerical constants in the equations.)

OUTLOOK

This paper has presented some interesting aspects of bubble-formation phenomena and has, it is hoped, pointed out some areas in which theoretical analysis might be fruitful. It would seem that the study of the liquid behavior at the orifice, including the creation of vortex rings and currents of liquid by the emerging bubbles, might hold the key to greater understanding of the curious phenomena associated with the formation of gas bubbles at orifices.

ACKNOWLEDGMENT

The work reported in this paper was made possible through the generosity of the donor of the Samuel Willard Bridgham Fellowship at Columbia University.

NOTATION

a = bubble radius (radius of spherical bubble of equal volume), cm.
c = speed of sound, cm./sec.
g = local acceleration of gravity, cm./sec.^{2}
h = distance through which a body has fallen from rest, cm.
K = constant coefficient in Equation (4)
K' = numerical constant
n = bubble frequency, bubbles/sec.
n_m = maximum bubble frequency, bubbles/sec.
N_c = "capacitance number" of orifice chamber, defined by Equation (3)
q = average gas-flow rate through orifice, cc./sec.
q_m = value of q at which maximum bubble frequency is reached, cc./sec.
r = orifice radius, cm.
u = velocity of a falling body, cm./sec.
v = bubble volume, cc.
v_e = theoretical hydrostatic bubble volume, based on Equation (1), cc.
V = rising velocity of bubbles in liquid, cm./sec.
V_b = volume of gas chamber below orifice, including piping, cc.
w = exponent as used in Equation (4)
ρ = density of liquid, g./cc.
ρ_g = density of gas, g./cc.
σ = surface tension of gas-liquid interface, dynes/cm.

LITERATURE CITED

1. Davidson, Leon, M.S. thesis, Columbia University, New York (1947).
2. ———, Ph.D. thesis, Columbia University, New York (1951); publication 3678, University Microfilms, Ann Arbor, Mich.
3. Eversole, W. G., G. H. Wagner, and Eunice Stackhouse, *Ind. Eng. Chem.*, **33**, 1459 (1941).
4. Geddes, R. L., *Trans. Am. Inst. Chem. Engrs.*, **42**, 79 (1946).
5. Guyer, August, and E. Peterhans, *Helv. Chim. Acta*, **26**, 1099 (1943).
6. Hagerty, P. F., II, M.S. thesis, Mass. Inst. Technol., Cambridge (1947).
7. Hughes, R. R., A. E. Handlos, H. D. Evans, and R. L. Maycock, *Chem. Eng. Progr.*, **51**, 557 (1955).

7a. *Ibid.*, p. 559.

8. Maier, C. G., *U. S. Bur. Mines Bull.* 260 (1927).
9. Peebles, F. N., and H. J. Garber, paper presented at Am. Inst. Chem. Engrs., Atlanta meeting (March, 1952).
10. Sprague, R. O., M.S. thesis, Columbia University, New York (1948).
11. van Krevelen, D. W., and P. J. Hoftijzer, *Chem. Eng. Progr.*, **46**, 29 (1950).
12. Wark, I. W., *J. Phys. Chem.*, **37**, 623 (1933).